



# The University of Bradford Institutional Repository

<http://bradscholars.brad.ac.uk>

This work is made available online in accordance with publisher policies. Please refer to the repository record for this item and our Policy Document available from the repository home page for further information.

To see the final version of this work please visit the publisher's website. Access to the published online version may require a subscription.

**Link to publisher version:** <https://doi.org/10.1039/c7sm01787a>

**Citation:** Swift T, Seaton CC and Rimmer S (2017) Poly(acrylic acid) interpolymer complexes. *Soft Matter*. 13(46): 8736-8744.

**Copyright statement:** © 2017 Royal Society of Chemistry. Full-text reproduced in accordance with the publisher's self-archiving policy.

## ARTICLE

## Poly(acrylic acid) Interpolymer Complexes

Thomas Swift<sup>\*a</sup>, Colin C. Seaton,<sup>a</sup> and Stephen Rimmer<sup>\* a</sup>

Cite this: DOI: 10.1039/x0xx00000x

Received 00th January 2012,  
Accepted 00th January 2012

DOI: 10.1039/x0xx00000x

www.rsc.org/

Interpolymer complex formation of poly(acrylic acid) with other macromolecules can occur via several mechanisms that vary depending on the pH. At low pH the protonated acid functional group can form bonds with both donor and acceptor moieties, resulting in desolvated structures consisting of two polymers. Complexes were formed in dilute solutions of PAA, functionalised with acenaphthylene, with a range of other polymers including: poly(NIPAM); poly(ethylene oxide) (PEO); poly(dimethylacrylamide) (PDMA); poly(diethyl acrylamide) (PDEAM) poly(vinyl alcohol) (PVA) and poly(vinyl pyrrolidone) (PVP). Fluorescence anisotropy was used to demonstrate complex formation in each case by monitoring the reductions in segmental motion of the chain as the complexes formed. Considerations of the molecular structures of the complexing moieties suggest that solvation energies and  $pK_a$ s play an important role in complex formation.

## Introduction

Hydrogen bonding is one of the most important factors to consider in the self-assembly of both natural and synthetic macromolecules<sup>1</sup>. However, even a comparatively simple polymer such as poly(acrylic acid) (PAA), a weak polyelectrolyte, experiences a range of other interacting forces (such as hydrophobic and ion-dipole interactions), which affect complex stability and can drive phase transitions<sup>2-4</sup>.

At low pH in dilute solution PAA forms an aggregated structure (previously, but inaccurately, described as a ladder or zipper structure<sup>5, 6</sup>, Fig 1) with several polyacrylamides<sup>7, 8</sup>. This is due to cooperative dual hydrogen bonding with both the protonated acid and the acrylamide amide proton acting as hydrogen bond donors<sup>9</sup>. This interaction must compete with hydrogen bonding with the solvent and the formation of intra-molecular carboxylic acid dimers. These interpolymer complexes (IPC) are rigid, static structures however they are susceptible to changing environmental conditions and even partial neutralisation of the polyacid is enough to inhibit complex formation<sup>10</sup>. Different complexes are affected to different degrees by changes in the environment: for example whilst the PAA bonds to poly(acrylamide) (PAM, primary amide backbone) are weakened by increasing temperature, both PAA – poly(*N*-isopropylacrylamide) (PNIPAM, secondary amide) and PAA – poly(dimethylacrylamide) (PDMA, tertiary amide) complexes are strengthened with temperature as this increases the strength of the hydrophobic interactions<sup>7, 11</sup>.

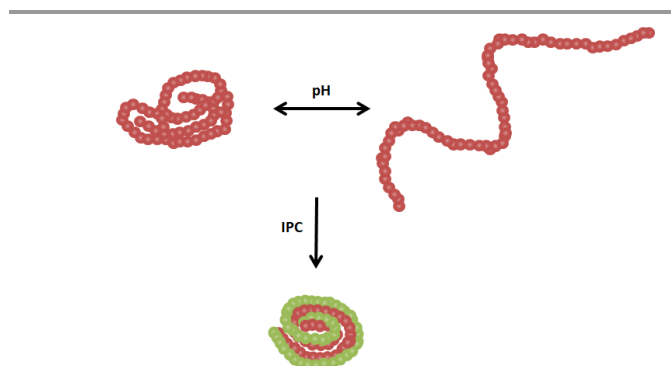


Fig. 1 – Poly(acrylic acid) switches between collapsed (globular) conformation and extended (swollen) conformation with pH. When exposed to a suitable complexing polymer in suitable conditions it can form an IPC connected via hydrogen bonding between polymer backbones.

Water soluble polymers have a multitude of uses in a range of industries, often as the complex associative structures. These materials can be used to alter the rheology, purity or polarity of the solution<sup>12</sup>. Also, there is interest in sensors capable of recognising low concentrations of polymer pollutants, predominantly using turbidometric<sup>13</sup> or spectrophotometric techniques<sup>14</sup>. In this respect we recently outlined a sensor method for detecting PAM in low concentrations (in the ppm range) using time resolved anisotropy<sup>15</sup>, utilising the restricted motion of polymers following interpolymer complexation with a fluorescently labelled PAA probe<sup>16, 17</sup>. PAM is an important industrial polymer due to its use in a range of industrial applications including wastewater treatment and oil purification<sup>18</sup> and as such was identified as a priority for environmental monitoring<sup>19</sup>. Concern over the use of PAM in particular is derived from the risk of residual monomer

spreading through the environment<sup>20</sup> and the danger of the soluble polymer to aquatic fauna<sup>21</sup>. However, minimisation of all forms of chemical fallout from industrial processes is desirable. The poly(acrylic acid-*co*-acenaphthylene) probe used in previous studies is capable of forming IPCs with a range of different polymer types other than PAM and so extension of the work for the detection of other polymer systems is of interest.

Fluorescence spectroscopy is an excellent technique for studying the transition of single molecules in dilute solutions<sup>5, 22-24</sup>. A range of fluorescence techniques have been considered to study these interactions in more detail. Typically the fluorophore is either dispersed in the polymer component<sup>25</sup> or covalently bound to the polymer backbone<sup>15, 19, 22</sup>. The benefit of the latter approach is that the fluorophore reports directly on the polymer backbone<sup>23, 24</sup>, although the loading of label should be taken into account as not to directly affect the properties of the homopolymer being investigated<sup>22</sup>. Primarily a low concentration of a single fluorophore, ACE, is included in the polymerisation mixture at loading below 1 % of the monomer feed to ensure the impact of the label on solution properties is minimal<sup>24</sup>. The anisotropy of this label has been shown to reflect the conformational state of the polymer<sup>24, 26</sup> and the system provides a substantial response if the polymer is engaged in interpolymer complexation<sup>15, 27</sup>. Time resolved anisotropy studies (TRAMS) are an excellent way of studying polymer mobility and the ACE label has been demonstrated as an excellent probe in this regard<sup>26, 28</sup>. There is no response of the fluorescence lifetime of the probe upon IPC formation<sup>15</sup>, as the complexed polymer shields the fluorophore from solvent just as effectively as the free collapsed PAA at low pH.

Complexation with a variety of water soluble polymers were studied. Many of these systems have previously been studied, and besides pH IPC binding can vary depending on both-temperature, concentration, molar mass and ionic strength<sup>2-8</sup>. For this study we have measured dilute solutions (0.1-0.5 mg ml<sup>-1</sup>), at low ionic strength at room temperature (18-22 °C) to ensure results are comparable. As the properties of these synthetic macromolecules depend on the basicity of their functional monomers a full understanding of their properties is essential to explain their solution behaviours. However despite substantial research in this field<sup>4, 29-33</sup> full solution behaviour of substituted amide functional groups are not documented in the current literature. To accommodate for this computational modelling experiments have been carried out to predict the properties of amide functional groups.

## Results and Discussions

### Polymer Synthesis

Both poly(acrylic acid) and acrylamide polymers were synthesised by free radical polymerisations in 1,4-Dioxane using AIBN as the initiator. In Table 1 the molar masses of these polymers are compared using size exclusion chromatography. It is clear that inclusion of ACE, with a comparable concentration of initiator, inhibited the polymerisation of acrylic acid and this resulted in lower apparent molar masses. The other polymers used were purchased premade from suppliers.

Table. 1 – Molecular weights of synthesised polymers determined by size exclusion chromatography<sup>a</sup>

Polymer	M <sub>n</sub> <sup>b</sup>	M <sub>w</sub> <sup>b</sup>	M <sub>z</sub> <sup>b</sup>	Đ
PAA	58,100	112,550	186,450	1.9
P(AA- <i>co</i> -ACE)*	42,150	64,900	89,950	1.5
PAM	19,700	47,900	114,700	2.4

<sup>a</sup>Stated molecular weights on supplied polymers were 100,000. <sup>b</sup>Molecular weights quoted as g mol<sup>-1</sup> \*Monomer feed of ACE less than 1% of copolymer random composition.

### Interpolymer Complexation with water soluble polymers

PAA binds to a range of polymers via repetitive hydrogen bonds across the polymer backbone as illustrated in Figure 2. Acrylamide based polymers including PAM, poly(ethyl acrylamide) (PEAM), poly(N-isopropylacrylamide) (PNIPAM), poly(dimethyl acrylamide) (PDMAM) and poly (diethyl acrylamide) (PDEAM) can each form dual hydrogen bonds with the carboxylic acid group of PAA. Poly(N-vinyl pyrrolidone) (PVP) forms a more constrained dual hydrogen bond that is dependent on the correct orientation of the acid, although the strength of binding is increased by hydrophobic interactions<sup>2</sup>. Poly(hydroxyethyl acrylamide) (PHEAM) can potentially complex through both the acrylamide and hydroxyl groups to PAA. To study these additional non-acrylamide effects single hydrogen bonding complexing partners were examined, include poly(acrylonitrile) (PACN), poly(ethylene oxide) (PEO) and poly(vinyl alcohol) (PVA).

Historically these hydrogen-bonding IPC have been represented in the style of a ladder/ribbon model<sup>9</sup>. Structures of binding-polymer complexes have been both extensively studied<sup>5, 6</sup> and modelled<sup>34</sup> in recent years indicating that they can adapt to a range of structures depending on conditions. The key interactions that form these polymer complexes are hydrogen bondings and with this in mind Figure 2 shows likely hydrogen bonding structures that should be considered for the various polymers at the repeat unit length scale.

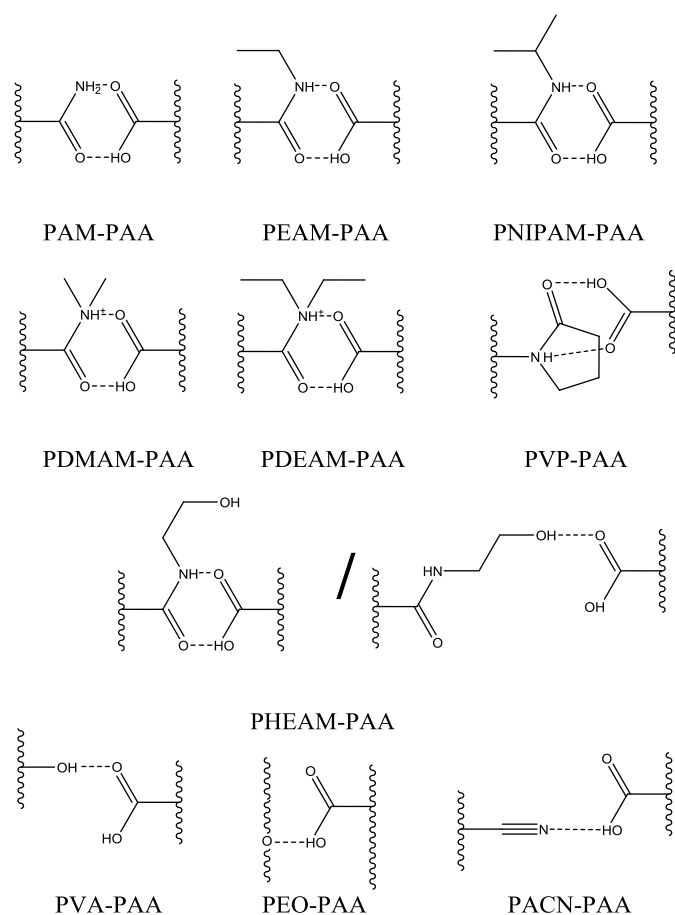


Fig. 2 – Proposed mode of hydrogen bonding interactions for interpolymer complexes.

Interpolymer complexation can be demonstrated by a number of techniques. Most common and easily used at high concentration is turbidimetry, although solid state NMR<sup>9</sup>, isothermal titration, potentiometry and viscometry have also been employed<sup>11</sup>. Although these samples aggregate over time, the complexes provided particles were sufficiently colloidally stable to allow particle sizing to be carried out to demonstrate the gross changes on complexation<sup>6</sup>. Dilute acidic solutions of non-complexed polymers do not give a strong light scattering signal and therefore calculated particle sizes were subject to large standard errors. However, the complexed polymers (which form aggregated suspensions) provided much more intense scattering of light and the particle size averages were more precise. Figure 3 shows the distribution of particle sizes obtained for all tested hydrogen bonding complexed polymers. Upon complexation with PAA (estimated particle size  $7.1 \pm 0.41$  nm) with PAM ( $6.03 \pm 1.12$  nm) the particles form a suspension, which more efficiently scatters light and the average particle diameter was found to be  $540 \pm 51$  nm. This demonstrates that aggregates of complexed particles were suspended in the mixture. Similarly in Figure 3 comparisons were also made between the PNIPAM, PDMA, PVP, PVA and PEO polymers alone and in the presence of PAA. In each case

the dissolved polymers had particle diameters of  $< 20$  nm and the complex formed particles that had significantly ( $p < 0.05$ ) larger sizes compared to the dilute single component solutions. The dual hydrogen bonding complexes (formed from PNIPAM, PDMA and PAM) provided aggregated particles of greater size than single hydrogen bonding complexes (PEO and PVA). PVP produced particles of intermediate sizes, possibly due to hindered sterics of bonding. In conclusion particle sizing offers independent evidence of IPC formation compared to fluorescence experiments. Particle sizing was also used to examine the colloidal stability of the suspended particles. These experiments showed that the dispersions tested after 3 hours were indistinguishable to those produced immediately after mixing.

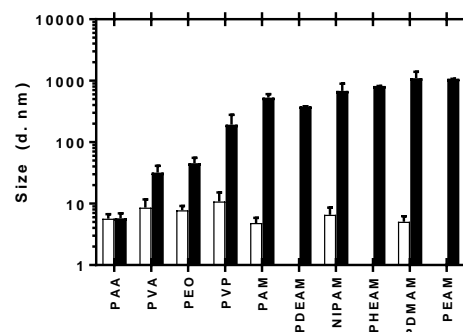


Fig. 3 – Histogram of mean particle diameters of polymers alone (white) and mixed with eq. concentration of PAA (black).

The anisotropy of the fluorescence of the ACE attached to the polymer backbone is defined as, shown in Equation 1:

$$r = \frac{I_{\parallel} - I_{\perp}}{I_{\parallel} + 2I_{\perp}} \quad \text{Equation 1}$$

Where  $I_{\parallel}$  is the intensity of the parallel and  $I_{\perp}$  is the intensity of the crossed polarised emissions.

The decay in  $r$  with time then provides a correlation time,  $\tau_c$ , as shown in equation 2 and 3:

$$r(t) = A \exp(-t / \tau_{c1}) + B \exp(-t / \tau_{c2}). \quad \text{Equation 2}$$

$$\tau_c = \frac{A\tau_{c1}^2 + B\tau_{c2}^2}{A\tau_{c1} + B\tau_{c2}} \quad \text{Equation 3}$$

Where  $A$  and  $B$  are constants and  $t$  is the measurement time. Full details are shown in the experimental and supporting information.

Labelled interpolymer complexes can be studied by fluorescence anisotropy<sup>15</sup>. An increase in  $\tau_c$  arises from a reduction in the decay of anisotropy as the rate of rotation of the chain segments is reduced. Therefore, determining  $\tau_c$  in the

absence and presence of complexing polymers can be used to examine the nature of the complexes at various pH.

Figure 4 shows the  $\tau_c$  data derived from the decays in anisotropy over a range of pH for mixtures of PAA and PEO, PACN or PVA. The data showed that  $\tau_c$  increased in P(AA-co-ACE) after exposure to receptive single hydrogen bonding polymers compared to dissolved P(AA-co-ACE) alone. However, the increase was only observed below a critical pH,  $pH_{crit}$ , which has been calculated via an  $EC_{50}$  (concentration of polymer added to give 50% maximal response) dose-response fit of the dataset. Below  $pH_{crit}$  there was an increase in  $\tau_c$  when the complexes were formed that at maximum extent was an increase of around 8-fold. This is a smaller change than that previously observed with a dual hydrogen bonding system; with PAM ( $pH_{crit}$  2.5)<sup>15</sup>.  $pH_{crit}$  for PVA is 3, whilst for PACN it is pH 2.4 and for PEO it was approximately pH 4.5. The observation of variations in  $pH_{crit}$  implies that the critical extent of the bonding within the complex is also different. The pH at which  $\tau_c$  occurs could be rationalised by considering that the extent of hydrogen bonding was related to the state of deionisation of the PAA and the base strength of the hydrogen bond acceptor polymer. The typical  $pK_a$  of a protonated primary alcohol (PVA) or a protonated ether (PEO) are  $pK_a$  -2.4 and -3.6 respectively<sup>29, 35</sup> whilst a protonated nitrile is around -12<sup>36</sup>. It can be considered that complex formation is dependent on the  $pK_a$  of the hydrogen bond receptor polymer so that the less basic PEO polymer forms a complex when the PAA is in a less protonated state ( $pH_{crit}$  4.5) than is required for more basic PVA ( $pH_{crit}$  3). This is further increased with respect for PACN. In our previous paper<sup>15</sup> we also showed that PAM forms a complex with PAA at pH 2.5; i.e. lower than the  $pH_{crit}$  observed for PVA. Primary amides are more basic than primary alcohols (amide- $H^+$   $pK_a$  -0.5)<sup>30, 37</sup>. Thus, the data on this set of polymers implies that the  $pH_{crit}$  might be related to the basicity of the hydrogen bond receptor; as the basicity of the acceptor increases a higher degree of protonation of the carboxyl groups, more extensive hydrogen bonding, is required to form the complex. Comparison of the change in  $\tau_c$  showed that complex formation is accompanied by a substantial increase in  $\tau_c$  at the  $pH_{crit}$ , which is not observed in P(AA-co-ACE) alone. The increase in  $\tau_c$  reflects a decrease in segmental mobility.

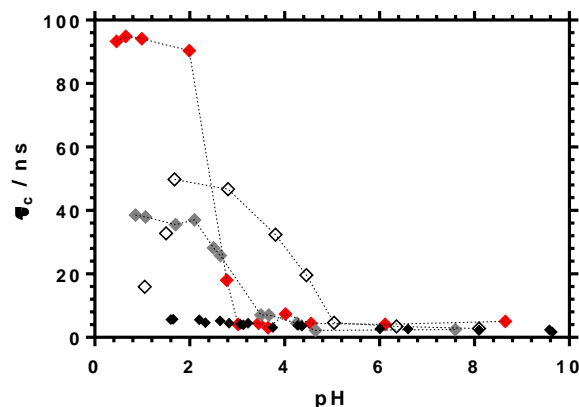


Fig. 4 – Correlation time of PAA ( $0.15 \text{ mg ml}^{-1}$ ) and single hydrogen bonding polymers ( $0.5 \text{ mg ml}^{-1}$ ) with varying pH. Polymers are PACN ( $\blacklozenge$ ), PEO ( $\diamond$ ) and PVA ( $\blacklozenge$ ). Included is PAA alone (uncomplexed -  $\blacklozenge$ ). Dotted lines show data points used in  $EC_{50}$  calculations.

The  $\tau_c$  of amide functional polymers were determined across the pH range and each of these demonstrated much greater increases, compared to PVA and PEO, in  $\tau_c$  below  $pH_{crit}$  as shown in Figure 5A, 5B and Figure 6.

Figure 5A compares the behaviour of PAM and three monoalkylated polyacrylamides (PEAM, PNIPAM and PHEAM) when complexed with PAA at various pH. The  $pH_{crit}$  was observed at pH 2-3 for PAA-PAM and PAA-PHEAM, and 3-5 for PAA-PEAM and PAA-PNIPAM. Thus, alkylation had the effect of shifting the  $pH_{crit}$  to a less acidic range. However, further functionalisation by addition of the hydroxyl group to PEAM (giving PHEAM) had the effect of shifting  $pH_{crit}$  to a more acidic range that was similar to the non-alkylated polymer; PAM. The data indicated that a strong effect of the solvation of the acrylamide units. That is the hydrophilic acrylamide group is expected to be more extensively solvated than the PEAM and PNIPAM units. Thus complex formation with PAM required a more highly protonated PAA state to form the complex. Then modification of the PEAM with the hydroxyl group (PHEAM) would be expected to increase solvation so that this polymer formed a complex only when the PAA was in the more protonated state compared to the state that could form a complex with PEAM. Fig 5B shows comparative data for dialkylated polymers PDMAM (poly(dimethylacrylamide)) and PDEAM (poly(diethylacrylamide)) which both exhibit higher  $pH_{crit}$  in line with hydrophobicity. Together this data indicates the effect of increasing alkylation of the amide on  $pH_{crit}$  by comparing a primary amide (PAM) to mono and di substituted acrylamides. The data indicated that  $pH_{crit}$  for the non-alkylated amide is much lower than for either the mono or dialkylated analogues unless additional factors (hydroxy group on PHEAM), which would effect solvation, were present.

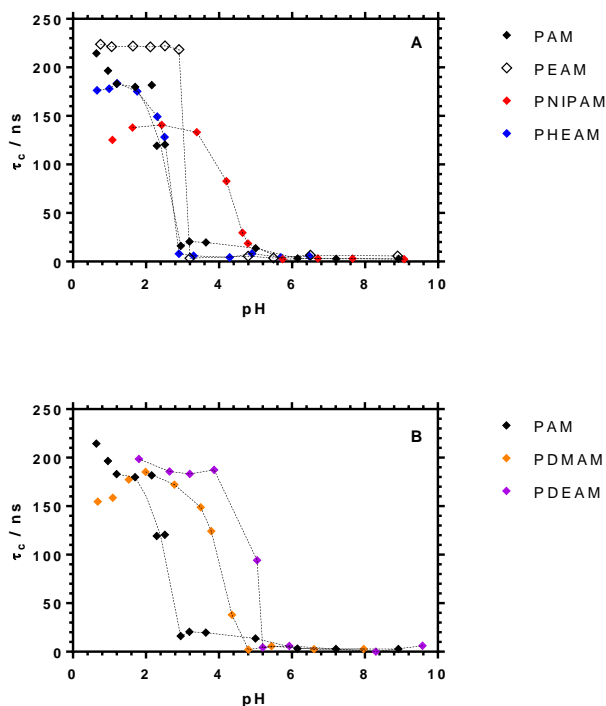


Fig 5 - Correlation time of PAA ( $0.15 \text{ mg ml}^{-1}$ ) and dual hydrogen bonding polymers ( $0.50 \text{ mg ml}^{-1}$ ) with varying pH. Polymers are PAM ( $\blacklozenge$ ) with monoalkylated series PEAM ( $\diamond$ ), PNIPAM ( $\blacklozenge$ ), PHMAM ( $\blacklozenge$ ) (A), and with increased alkylation polymers PDMAM ( $\blacklozenge$ ) and PDEAM ( $\blacklozenge$ ) (B). Lines show datapoints used in  $EC_{50}$  calculations.

PVP is a medically important material and is generally regarded as a safe polymer that was first used in aqueous solution as a blood substitute on battlefields. The polymer also contains substituted amide functionality but in the reverse orientation to the main chain compared to acrylamides. The PAA-PVP complexes were found to have a correlation time that varied across the entire pH range, with a gradual transition that occurred between pH 2 to 5 (Fig. 6). Thus, in this system the two polymer components appear to form a loose complex around pH 5. Then as the protonation of the PAA increased the complex became more well developed to pH 2.

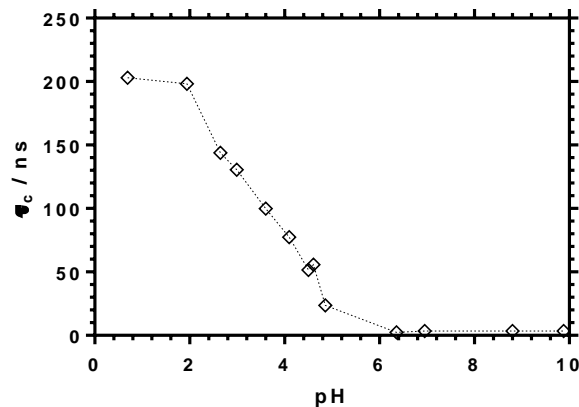


Fig 6 - Correlation time of PAA ( $0.15 \text{ mg ml}^{-1}$ ) and dual hydrogen bonding polymer PVP ( $0.50 \text{ mg ml}^{-1}$ ) with varying pH. Lines show data points used in  $EC_{50}$  calculations.

Hydrogen bonding to the proton accepting polymer (the polymer other than PAA) can be considered as an acid-base type of interaction described by the equilibrium constants;  $K_a$  or  $pK_a$  etc. Therefore, reviewing these data it is tempting to suggest that considering the  $pK_a$  of the accepting polymer and the factors that contribute to this parameter would be responsible for the differences in  $pH_{crit}$ . However the appropriate values for mono and dialkylated amides are not readily available<sup>29, 30, 37</sup>. On the other hand differences in the solvation of the amide groups would also offer an explanation for the differences in  $pH_{crit}$ ; that is more extensive hydrogen binding (at lower  $pH_{crit}$ ) would be required to form the complex as the solvation of the proton accepting polymer increased. Therefore, in order to examine either of these hypotheses, computational models were developed.

### Computational Study

As the experimental  $pK_a$  values are unknown for some of these systems, a computational investigation was undertaken to predict the values and identify any possible structural reason for the trend displayed in the experimental results. Accurate prediction of  $pK_a$  values requires time consuming high-level theory calculations<sup>38</sup>, however experimental  $pK_a$  values can be used to correct the lower quality results of a faster density functional theory calculation since the error is systematic in solvation of ionic species.<sup>39</sup>

Calculations using this methodology (Supp. Info) were carried out on the seven amide monomer structures considering the protonated molecules (Figure 7). Optimisation of N protonated systems often indicated instability in the molecule and so only the results relative to the O protonated systems were considered. Selected systems were tested as vinyl monomer to confirm the influence of this choice. Vinyl alcohol and ethylene glycol repeat units were also considered to confirm the effectiveness of the calculation while a set of structurally

similar molecules were used to generate a correction curve for the calculated  $pK_a$ s (SI. Table S1).

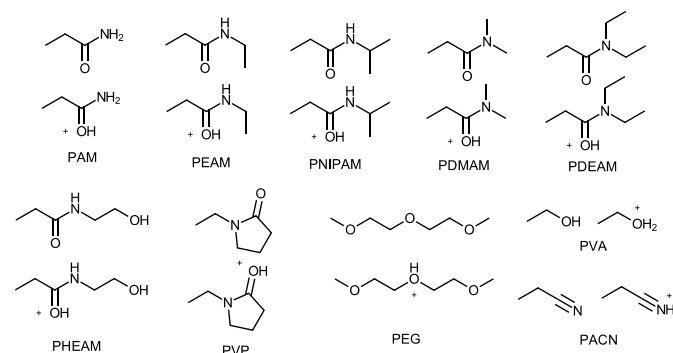


Fig. 7 – Chemical structures of the systems used in the calculations.

The results (Table 2) indicate weak acidity for all systems with negative  $pK_a$  values with a general trend to higher  $pK_a$  as the substitution increased on the nitrogen, although PNIPAM is anomalous. As these models only considered a single monomer unit within the repeated polymer segments, intramolecular interactions may alter their properties. To address this a subset of calculations on trimers were undertaken to confirm whether potential intramolecular interactions between repeat moieties would alter the protonation state of the system. Trimers for PAM, PEAM, PNIPAM and PDMAM were constructed and the systems optimised as for the monomers (Table 3). The protonation was modelled as occurring on the middle amide group. These results show similar trends to the monomer models and clearly indicated that all systems would be unprotonated at the pHs considered.

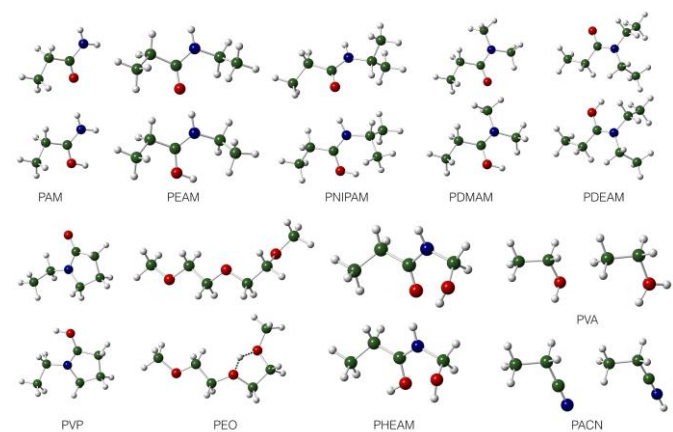


Fig. 8 – Comparison of the optimised structures obtained from each starting system shown in Fig. 6.

Table 2 Results of  $pK_a$  calculations on monomer models.  $pK_a$  correction calculated from best fit line to reference dataset (Corrected  $pK_a = 0.4967^*$  Calculated  $pK_a + 0.9184$ )

System*	Calculated $pK_a$	Corrected $pK_a$
PAM	-6.99	-2.55
PEAM	-6.66	-2.39
PNIPAM	-8.90	-3.51
PDMAM	-5.05	-1.59
PDEAM	-4.831	-1.486
PVP	-7.31	-2.72
PVA	-15.31	-6.70
PEG	-16.03	-7.06
PACN	-18.149	-8.113
PHEAM	-7.646	-2.886

\* $pK_a$  for monomer models not polymeric system

Table 3 Results of  $pK_a$  calculations for trimer models.  $pK_a$  values corrected as in Table 2.

System*	Calculated $pK_a$	Corrected $pK_a$
PAM	0.13	0.98
PEAM	-5.62	-1.88
PNIPAM	-4.02	-1.08
PDMAM	1.56	1.69

\* $pK_a$  for trimer models not polymeric system

Analysis of the components of the calculation indicated that the largest difference between the systems occurs in terms of the solvation energy of the neutral molecule (Table 4). The difference in Gibbs energy of solvation between the primary system and the others increased with increasing substitution. The behaviour of the polymers falls into three classes: primary (acrylamide) had  $pH_{crit}$  2.1 to 3.0; secondary, ternary amides (isopropyl and ethyl acrylamide and dimethyl and diethyl acrylamide) and PEG had higher  $pH_{crit}$  3.5 to 5.0 and PVA had  $pH_{crit}$  3. The third class, the cyclic amide (pyrrolidinone), provided a broader  $pH_{crit}$  range between  $pH$  2.0 to 5.0. For amides, in the monomer and trimer calculations the solvation energies are also clustered in this manner. That is the solvation energy of the primary amide is clearly predicted to be higher than the secondary and ternary amides.  $pH_{crit}$  for PEG is similar to the secondary and ternary amides and the solvation energies are also similar. From these calculations the solvation energies appear to be useful guides to the  $pH$  mediated complex behaviour of these amide polymers. However, the relationship between  $pH$  and solvation energy for the PAA-PVA complex appeared to be anomalous. This complex formed at  $pH_{crit}$  3 but the solvation energy was the lowest. This observation could be rationalised by considering that PVA readily forms intrachain and interchain hydrogen bonds so<sup>40</sup> that complex formation becomes favourable only at high degrees of protonation of the PAA component; when there is increased probability of forming hydrogen bonds between vinyl alcohol and acrylic acid units.

There was a clear trend in the solvation energies for the non-protonated monomers and trimers. In water solvation is dominated by hydrogen bonding and hydrophobic effects. The



simulations and the experimental data suggest that for the more highly solvated systems (higher solvation exotherm) increased hydrogen bonding capacity is required to form the IPC.

Table 4. Comparison of calculated solvation energies for neutral molecule in the monomer and trimer system.  $\Delta\Delta G^{\circ}\text{aq} = \Delta G^{\circ}\text{aq}(\text{primary}) - \Delta G^{\circ}\text{aq}$

System	$\Delta G_{\text{sol}}/\text{kJ}\cdot\text{mol}^{-1}$	$\Delta\Delta G_{\text{sol}}/\text{kJ}\cdot\text{mol}^{-1}$
PAM Monomer	-44.802	0.0
PEAM Monomer	-39.624	-5.178
PNIPAM Monomer	-38.902	-5.900
PDMAM Monomer	-34.828	-9.974
PDEAM Monomer	-32.113	-12.689
PVP Monomer	-37.951	-6.851
PVA Monomer	-23.029	-21.773
PEO Monomer	-35.079	-9.723
PACN Monomer	-30.368	-14.434
PHEAM Monomer	-44.705	-0.097
PAM Trimer	-105.526	0.0
PEAM Trimer	-83.087	-22.439
PDEAM Trimer	-63.038	-42.488
PNIPAM Trimer	-76.114	-29.412
PDMAM Trimer	-60.827	-44.699

Considering the computational data presented a pattern emerges indicating that the energy of solvation of a polymer backbone may dictate the observed  $pH_{\text{crit}}$  that governs interpolymer complexation. With the exception of PAA – PVA / PEO complexes, which operate via a single bonding site system, there is a common trend in acid proton-receiving polymers exhibiting a higher  $pH_{\text{crit}}$  if the solubilisation energy is lower (Fig. 9). Noticeable deviations from this trend are found with PNIPAM whose  $pH_{\text{crit}}$  is higher but solubilisation energy smaller than other secondary and tertiary amines. This could be related to the lower-critical solution temperature responsiveness of the polymer system which will not be found in monomeric systems. PHEAM lies in line with this trend despite the potential for additional binding via the hydroxy group.

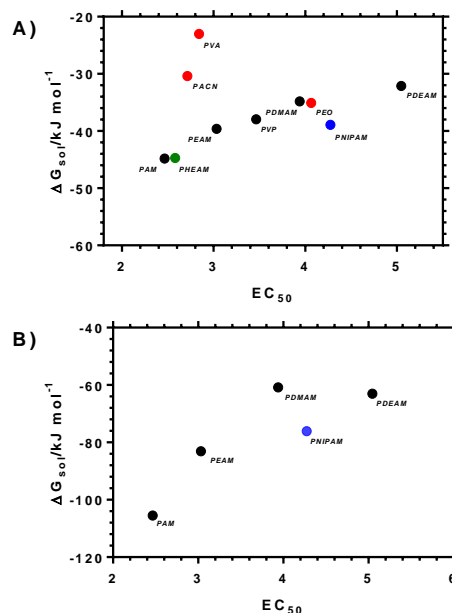


Fig. 9 –  $EC_{50}$  values determined from decrease in  $\tau_c$  compared to calculated  $\Delta G^{\circ}\text{aq}$  of A) monomer and B) trimer systems. Non alk-amide datapoints indicated include single bonding site complexes (red), PNIPAM (blue) and PHEAM (green).

## Conclusions

The formation of IPC complexes between PAA and a range of other polymer systems has been demonstrated utilising the fluorescence anisotropy of an AA copolymer containing a naphthalene comonomer. IPC formation was dependant on the  $pH$  and each individual IPC displayed a defined critical maximum  $pH$  for formation,  $pH_{\text{crit}}$ . The observation of a  $pH_{\text{crit}}$  and simulations showed that the state of ionisation of the PAA and solvation energies of the acceptor polymer defined the formation of an IPC.

## Experimental

### Materials

All materials were used as supplied and sourced from Sigma-Aldrich unless otherwise stated. The fluorescent label ACE was purified via column chromatography in methanol before use.

### Synthesis

Linear polymers were synthesised by dissolving distilled monomer and 4,4'-azobis(isobutyronitrile) (AIBN) in dioxane. Samples were thoroughly degassed via three freeze-pump-thaw cycles. Once oxygen had been removed from the system the ampoules were flame sealed and heated to 60°C in a water bath for three days. Afterwards the precipitated polymer was filtered, dissolved in deionised water and added to rapidly stirring butanol to purify. After repeated purification steps the samples were left in a vacuum oven until dry. Poly(acrylamide)



<sup>1</sup>H NMR in D<sub>2</sub>O (δ 2.31 (m CH) δ 1.99 (m CH<sub>2</sub>) δ 1.6 (m CH<sub>3</sub>)). <sup>13</sup>C NMR in D<sub>2</sub>O (δ 180 ppm (s CONH<sub>2</sub>) δ 41 ppm (CC(CONH<sub>2</sub>)C) δ 32 ppm (CCH<sub>2</sub>C)). Poly(acrylic acid) <sup>1</sup>H NMR in D<sub>2</sub>O (δ 2.35 (m CH) m (δ 1.75 CH<sub>2</sub>))<sup>19</sup> <sup>13</sup>C NMR in D<sub>2</sub>O (δ 180 ppm (s COOH) δ 41 ppm (CC(COOH)C) δ 35 ppm (CCH<sub>2</sub>C)).

Table. 6 Relative Monomer feed\*

Polymer	AA	AIBN	ACE
PAA	100	0.87	-
P(AA-co-ACE)	100	0.88	0.52
PAM	100	0.85	-

\*All monomer feeds given as a comparable ratio to moles of acrylic acid.

### Polymer Characterisation

Polyacrylamide samples were analysed by size exclusion chromatography (SEC) at room temperature using a high molecular weight column setup consisting of 2x300mm TSKgel GMPWxl columns. All samples were run using aqueous solution mobile phase of 0.1 M sodium nitrate and 0.01 M sodium dihydrogen phosphate. Samples were prepared up to 1 mg ml<sup>-1</sup> and injected using a Rheodyne 200 μm injection loop. The samples were analysed using a refractive index (RI) detector (HP 1047A RI Detector), calibrated to give polymer molecular weights calculated from the known retention time of standard PEG/PEO polymers.

To obtain molar masses by SEC the acidic samples were modified via a methylation reaction with trimethylsilyldiazomethane. The product was then dissolved in THF (solvent filtered by 0.45 μm pore). A Kinesis 307 Gilson Pump passed the sample through 3x PLgel 10 μm mixed-B columns at 1.00 ml min<sup>-1</sup> flow rate. Samples were added via a Anachem 234 auto injector and the RI signal was recorded using an Erma Inc. ERC-7512 RI detector. The system was calibrated using PMMA samples.

The particle size of the polymers was measured using a Malvern Zetasizer Nanoseries Nano-ZS operating at a dual angle system. A dilute (1 mg ml<sup>-1</sup>) solution of polymer in ultrapure water was loaded in a 1 cm path length cuvette and studied at 25 °C. Each sample was measured several times over multiple runs with a measurement time of 10s per run and the particle size determined by volume averaging using Zetasizer software. Comparison between samples was carried out using a nonparametric Mann Whitney test.

Steady state spectra were recorded on a Fluoromax-4 Spectrofluorometer (HORIBA Scientific) with an excitation/emission slit width of 1 nm. All solutions were recorded in 1 cm quartz cuvettes with sample concentrations < 1 mg ml<sup>-1</sup> in ultrapure water.

Fluorescence time resolved lifetime and anisotropy measurements were recorded using an Edinburgh Instruments 199 Fluorescence Spectrometer at an excitation wavelength of 295 nm and the emission wavelength of 340 nm. Measurements were made across 512 channels representing a 200 nanosecond time period. The profile of the laser beam was monitored using a silica prompt to scatter light at the excitation wavelength. All solutions were examined in quartz cuvettes with a path length of 10 mm and then the emitted light was passed through a polariser that rotated between two 90° angles every 30 seconds. The extent of the difference between polarisations is described in terms of anisotropy (*r*), which arises from the relative intensities of the parallel (*I*<sub>||</sub>) and crossed (*I*<sub>⊥</sub>) polarised emissions. The G factor (instrument sensitivity towards vertically and horizontally polarized light) of the device was calculated to be 1.0004, with a standard deviation of 0.0111. This indicates that light polarized in a vertical and horizontal direction was detected equally. As the G factor was close to unity Equation 1 can be considered to calculate the anisotropy, *r*. The change in the instrumentally measured anisotropy function, *r*(*t*), over time was then fitted to two scaling factors (A and B) and two correlation time components (τ<sub>c1</sub> and τ<sub>c2</sub>). The fitting process was carried out using Horiba Scientific Software Datastation using Equation 2:

From equation 2 the correlation time of the sample, τ<sub>c</sub>, is determined by Equation 3:

$$\tau_c = \frac{A\tau_{c1}^2 + B\tau_{c2}^2}{A\tau_{c1} + B\tau_{c2}} \quad \text{Equation 3}$$

The quality of the fit of the decay was indicated both by the standard deviation of the fit and the χ<sup>2</sup> quality of fit. Considering complexation studies of polymeric P(AA-co-ACE) both A and τ<sub>c1</sub> have been fixed to constant values<sup>15</sup> to represent the uncomplexed probe polymer so B and τ<sub>c2</sub> are left variable to represent the contributions from complexing molecules<sup>19</sup>. Error bars are given as one standard deviation of the single measurement gathered from at least 20,000 data points. Full analytical details are contained within the ESI.

EC<sub>50</sub> values (concentration of polymer added to give 50% maximal response) were calculated in Graphpad Prism V7.02).

### Computational Studies

Calculations on molecular structures were carried out comparing a neutral and two protonated variants of the monomer. Each molecule was initially structurally optimised by DFT methods (PBE-D3/TZV(2d) non H atoms, TZV(p) H atoms).<sup>41-44</sup> The thermodynamic properties at 298.15 K of the optimised structures were then evaluated at the B3LYP-D3/def2-TZVPPD level<sup>45</sup> in both the gas phase and aqueous solution using the COSMO methodology.<sup>46</sup> All calculations were carried out in the program orca.<sup>47</sup>

### Acknowledgements

Synthetic work was carried out as part of an EPSRC CASE funded PhD studentship at the University of Sheffield,

sponsored by SNF (UK) Ltd (award EP/H501541/1). We'd like to thank Frederick Marshall for assistance with sample preparation for Fluorescence Measurements.

## Notes and references

<sup>a</sup> School of Chemistry and Biosciences, University of Bradford, Bradford, West Yorkshire, BD7 1DP, UK. E-mail: s.rimmer@bradford.ac.uk;

† Footnotes should appear here. These might include comments relevant to but not central to the matter under discussion, limited experimental and spectral data, and crystallographic data.

Electronic Supplementary Information (ESI) available: Computational raw data, calibration of  $pK_a$  calculations, Analysis of Fluorescence Labels, raw anisotropy data and particle size data. See DOI: 10.1039/b000000x/

1. Stross, A. E.; Iadevaia, G.; Hunter, C. A., Cooperative duplex formation by synthetic H-bonding oligomers. *Chemical Science* **2016**.
2. Vasheghani Farahani, B.; Hosseinpour Rajabi, F.; Ahmadi, M. H.; Zenooz, N., Qualitative Investigation on some H-bonded Interpolymer Complexes by Determination of Thermodynamic Parameters. *Journal of the Mexican Chemical Society* **2012**, *56*, 212-216.
3. Biswas, S.; Mani, E.; Mondal, A.; Tiwari, A.; Roy, S., Supramolecular polyelectrolyte complex (SPEC): pH dependent phase transition and exploitation of its carrier properties. *Soft Matter* **2016**.
4. Nurkeeva, Z. S.; Mun, G. A.; Dubolazov, A. V.; Khutoryanskiy, V. V., pH Effects on the Complexation, Miscibility and Radiation-Induced Crosslinking in Poly(acrylic acid)-Poly(vinyl alcohol) Blends. *Macromolecular Bioscience* **2005**, *5*, 424-432.
5. Swift, T.; Paul, N.; Swanson, L.; Katsikogianni, M.; Rimmer, S., Förster Resonance Energy Transfer across interpolymer complexes of poly(acrylic acid) and poly(acrylamide). *Polymer* **2017**, *123*, 10-20.
6. Deng, L.; Wang, C.; Li, Z.-C.; Liang, D., Re-examination of the "Zipper Effect" in Hydrogen-Bonding Complexes. *Macromolecules* **2010**, *43* (6), 3004-3010.
7. Sudre, G.; Tran, Y.; Creton, C.; Hourdet, D., pH/Temperature control of interpolymer complexation between poly(acrylic acid) and weak polybases in aqueous solutions. *Polymer* **2012**, *53* (2), 379-385.
8. Bizley, S. C.; Williams, A. C.; Khutoryanskiy, V. V., Thermodynamic and kinetic properties of interpolymer complexes assessed by isothermal titration calorimetry and surface plasmon resonance. *Soft Matter* **2014**, *10* (41), 8254-8260.
9. Garces, F. O.; Sivadasan, K.; Somasundaran, P.; Turro, N. J., Interpolymer complexation of poly(acrylic acid) and polyacrylamide: structural and dynamic studies by solution- and solid-state NMR. *Macromolecules* **1994**, *27* (1), 272-278.
10. Staikos, G.; Bokias, G.; Tsitsilianis, C., The viscometric methods in the investigation of the polyacid-polybase interpolymer complexes. *Journal of Applied Polymer Science* **1993**, *48* (2), 215-217.
11. Staikos, G.; Karayanni, K.; Mylonas, Y., Complexation of polyacrylamide and poly(N-isopropylacrylamide) with poly(acrylic acid). The temperature effect. *Macromolecular Chemistry and Physics* **1997**, *198* (9), 2905-2915.
12. Winnik, M. A.; Yekta, A., Associative polymers in aqueous solution. *Current Opinion in Colloid & Interface Science* **1997**, *2* (4), 424-436.
13. Kang, J.; Sowers, T. D.; Duckworth, O. W.; Amoozegar, A.; Heitman, J. L.; McLaughlin, R. A., Turbidimetric Determination of Anionic Polyacrylamide in Low Carbon Soil Extracts. *J. Environ. Qual.* **2014**, *42* (6), 1902-1907.
14. Al Momani, F. A.; Örmeci, B., Measurement of polyacrylamide polymers in water and wastewater using an in-line UV-vis spectrophotometer. *Journal of Environmental Chemical Engineering* **2014**, *2* (2), 765-772.
15. Swift, T.; Swanson, L.; Rimmer, S., Poly(acrylic acid) interpolymer complexation: use of a fluorescence time resolved anisotropy as a poly(acrylamide) probe. *RSC Advances* **2014**, *4* (101), 57991-57995.
16. Heyward, J. J.; Ghiggino, K. P., Fluorescence polarization study of the poly(acrylic acid)/poly(ethylene oxide) interpolymer complex in aqueous solution. *Macromolecules* **1989**, *22* (3), 1159-1165.
17. Soutar, I.; Swanson, L., Luminescence Studies of Polyelectrolyte Behavior in Solution. 3. Time-Resolved Fluorescence Anisotropy Measurements of the Conformational Behavior of Poly(methacrylic acid) in Dilute Aqueous Solutions. *Macromolecules* **1994**, *27* (15), 4304-4311.
18. Bolto, B.; Gregory, J., Organic polyelectrolytes in water treatment. *Water Research* **2007**, *41* (11), 2301-2324.
19. Swift, T.; Swanson, L.; Bretherick, A.; Rimmer, S., Measuring poly(acrylamide) flocculants in fresh water using inter-polymer complex formation. *Environmental Science: Water Research & Technology* **2015**, *1* (3), 332-340.
20. Touzé, S.; Guérin, V.; Guezennec, A.-G.; Binet, S.; Togola, A., Dissemination of acrylamide monomer from polyacrylamide-based flocculant use—sand and gravel quarry case study. *Environ Sci Pollut Res* **2014**, 1-8.
21. Harford, A. J.; Hogan, A. C.; Jones, D. R.; van Dam, R. A., Ecotoxicological assessment of a polyelectrolyte flocculant. *Water Research* **2011**, *45* (19), 6393-6402.
22. Ruiz-Pérez, L.; Pryke, A.; Sommer, M.; Battaglia, G.; Soutar, I.; Swanson, L.; Geoghegan, M., Conformation of Poly(methacrylic acid) Chains in Dilute Aqueous Solution. *Macromolecules* **2008**, *41* (6), 2203-2211.
23. Zhang, Q.; Vancoillie, G.; Mees, M. A.; Hoogenboom, R., Thermoresponsive polymeric temperature sensors with broad sensing regimes. *Polymer Chemistry* **2015**.
24. Swift, T.; Swanson, L.; Geoghegan, M.; Rimmer, S., The pH-responsive behaviour of poly(acrylic acid) in aqueous solution is dependent on molar mass. *Soft Matter* **2016**, (12), 2542 - 2549.
25. Plenderleith, R.; Swift, T.; Rimmer, S., Highly-branched poly(N-isopropyl acrylamide)s with core-shell morphology below the lower critical solution temperature. *RSC Advances* **2014**, *4* (92), 50932-50937.
26. Sparks, D. J.; Romero-Gonzalez, M. E.; El-Taboni, E.; Freeman, C. L.; Hall, S. A.; Kakonyi, G.; Swanson, L.; Banwart, S. A.; Harding, J. H., Adsorption of poly acrylic acid onto the surface of calcite: an experimental and simulation study. *Physical Chemistry Chemical Physics* **2015**, *17* (41), 27357-27365.
27. Soutar, I.; Swanson, L.; Thorpe, F. G.; Zhu, C., Fluorescence Studies of the Dynamic Behavior of Poly(dimethylacrylamide) and Its

- Complex with Poly(methacrylic acid) in Dilute Solution. *Macromolecules* **1996**, *29* (3), 918-924.
28. Soutar, I.; Swanson, L.; Cowie, J. M. G.; Barker, I. C.; Flint, N. J.; Conroy, M. J., Shedding light upon macromolecular behaviour: Luminescence studies of polymers. *Macromolecular Symposia* **1999**, *141* (1), 69-82.
29. Jencks, W. P.; Regenstein, J., Ionization Constants of Acids and Bases. In *Handbook of Biochemistry and Molecular Biology, Fourth Edition*, CRC Press: 2010; pp 595-635.
30. *Handbook of Chemistry and Physics*. Chemical Rubber Publishing Company: Cleveland, 1951.
31. Khutoryanskiy, V. V.; Dubolazov, A. V.; Nurkeeva, Z. S.; Mun, G. A., pH Effects in the Complex Formation and Blending of Poly(acrylic acid) with Poly(ethylene oxide). *Langmuir* **2004**, *20*, 3785-3790.
32. Mun, G. A.; Nurkeeva, Z. S.; Khutoryanskiy, V. V.; Sarybayeva, G. S.; Dubolazov, A. V., pH-effects in the complex formation of polymers I. Interaction of poly(acrylic acid) with poly(acrylamide). *European Polymer Journal* **2003**, *39*, 1687-1691.
33. Nurkeeva, Z. S.; Mun, G. A.; Khutoryanskiya, V. V.; Bitekenova, A. B.; Dubolazov, A. V.; Esirkegenova, S. Z., pH effects in the formation of interpolymer complexes between poly(N-vinylpyrrolidone) and poly(acrylic acid) in aqueous solutions. *The European Physical Journal E* **2003**, *10*, 65-68.
34. Alexei A. Lazutin; Alexander N. Semenov; Vasilevskaya, V. V., Polyelectrolyte Complexes Consisting of Macromolecules With Varied Stiffness: Computer Simulation. *21* **2012**, 328-339.
35. Evans Group pKa Table. [http://www2.lsddiv.harvard.edu/pdf/evans\\_pKa\\_table.pdf](http://www2.lsddiv.harvard.edu/pdf/evans_pKa_table.pdf) (accessed 11/06/2015).
36. Anslyn, E. V.; Dougherty, D. A., *Modern physical organic chemistry*. University Science Books: 2006.
37. Blake Peterson Group pKa Values, by W.P. Jencks and F. H. Westheimer. [http://research.chem.psu.edu/brpgroup/pKa\\_compilation.pdf](http://research.chem.psu.edu/brpgroup/pKa_compilation.pdf) (accessed 11/06/2015).
38. Liptak, M. D.; Gross, K. C.; Seybold, P. G.; Feldgus, S.; Shields, G. C., Absolute pKa Determinations for Substituted Phenols. *Journal of the American Chemical Society* **2002**, *124* (22), 6421-6427.
39. Muckerman, J. T.; Skone, J. H.; Ning, M.; Wasada-Tsutsui, Y., Toward the accurate calculation of pKa values in water and acetonitrile. *Biochimica et Biophysica Acta (BBA) - Bioenergetics* **2013**, *1827* (8-9), 882-891.
40. Sin, L. T.; Rahman, W. A. W. A.; Rahmat, A. R.; Samad, A. A., Computational modeling and experimental infrared spectroscopy of hydrogen bonding interactions in polyvinyl alcohol-starch blends. *Polymer* **2010**, *51* (5), 1206-1211.
41. Schäfer, A.; Horn, H.; Ahlrichs, R., Fully optimized contracted Gaussian basis sets for atoms Li to Kr. *The Journal of Chemical Physics* **1992**, *97* (4), 2571-2577.
42. Weigend, F.; Ahlrichs, R., Balanced basis sets of split valence, triple zeta valence and quadruple zeta valence quality for H to Rn: Design and assessment of accuracy. *Physical Chemistry Chemical Physics* **2005**, *7* (18), 3297-3305.
43. Grimme, S.; Antony, J.; Ehrlich, S.; Krieg, H., A consistent and accurate ab initio parametrization of density functional dispersion correction (DFT-D) for the 94 elements H-Pu. *The Journal of Chemical Physics* **2010**, *132* (15), 154104.
44. Grimme, S.; Ehrlich, S.; Goerigk, L., Effect of the damping function in dispersion corrected density functional theory. *Journal of Computational Chemistry* **2011**, *32* (7), 1456-1465.
45. Rappoport, D.; Furche, F., Property-optimized Gaussian basis sets for molecular response calculations. *The Journal of Chemical Physics* **2010**, *133* (13), 134105.
46. Klamt, A., The COSMO and COSMO-RS solvation models. *Wiley Interdisciplinary Reviews: Computational Molecular Science* **2011**, *1* (5), 699-709.
47. Neese, F., The ORCA program system. *Wiley Interdisciplinary Reviews: Computational Molecular Science* **2012**, *2* (1), 73-78.